Dielectric loss of half-doped manganite $La_{0.5}Ca_{0.5}MnO_3$*

Cao Xian-Sheng(曹先胜)[a)†], Ji Gao-Feng(吉高峰)[a)b)], Luo Bing-Cheng(罗炳成)[c)], and Li Feng(李 峰)[a)]

[a)] *School of Mathematics and Physics, Changzhou University, Changzhou* 213164, *China*
[b)] *Department of Microelectronics, State Key Laboratory of ASIC and Systems, Fudan University, Shanghai* 200433, *China*
[c)] *Shaanxi Key Laboratory of Condensed Matter Structures and Properties, School of Science, Northwestern Polytechnical University, Xi'an* 710072, *China*

(Received 8 December 2012; revised manuscript received 8 January 2013)

The dielectric loss tanδ of half-doped manganite $La_{0.5}Ca_{0.5}MnO_3$ is investigated using Green's function technique. The $La_{0.5}Ca_{0.5}MnO_3$ is described by the Kondo-lattice model in the double exchange limit, taking into account the Jahn–Teller distortion and the super-exchange interaction between the localized electrons. It is found that the intensity of tanδ decreases with increasing $|\varepsilon_{\rm JT}|$, V, and U. It is also observed that the transition temperature $T_{\rm P}$ rises as $|\varepsilon_{\rm JT}|$ and U increase. It is worth noting that $T_{\rm P}$ remains unchanged and the strength of tanδ increases with increasing g. The calculated dielectric loss results are explained theoretically, and these behaviors are in qualitative agreement with the experimental results.

Keywords: multiferroics, dielectric loss, $La_{0.5}Ca_{0.5}MnO_3$

PACS: 77.22.Gm, 77.84.Lf, 85.35.Ds **DOI:** 10.1088/1674-1056/22/8/087702

1. Introduction

The half-doped manganite $La_{0.5}Ca_{0.5}MnO_3$ (LCMO) has become a hot research topic again in recent years due to the rich underlying multiferroicity and magnetoelectric (ME) effects, as well as the great potential for technological applications.[1–3] Very recently, the peculiar multiferroics of the LCMO were experimentally verified by Zou *et al.*,[4] and Indu Dhiman *et al.*[5] experimentally studied the dielectric responses of $La_{0.5}Ca_{0.5-x}Sr_xMnO_3$ ($0.1 \leq x \leq 0.4$) manganites with different magnetic ground states. Recently, Giovannetti *et al.*[6] proposed theoretically that the combination of peculiar charge-orbital ordering tends to form a spin dimmer in LCMO, which breaks the inversion symmetry and results in polar states with relatively strong ferroelectricity. Generally, there are two kinds of theoretical research methods:[7] one is the first-principles calculation method, which is based on the density functional theory (DFT) and appears to be well suited to addressing some of the critical issues that are not easily accessible through experiments, such as the value of P and the structural and electronic mechanisms of ferroelectricity; and the other is the Hamiltonian modeling method, which is key to investigating the microscopic mechanisms on the basis of the multiferroic behavior in manganites. To our knowledge, only a small amount of theoretical work has been done on the dielectric loss of LCMO using microscopic Hamiltonian modeling.

In the present work, a quantum microscopic model is used to study the dielectric loss of the LCMO. The rest of this paper is organized as follows. The Hamiltonian of LCMO model is described in Section 2. The phonon Green function is calculated and the dielectric loss is also reported in Section 3. Finally, the results and discussions are given in Section 4. Some conclusions are drawn from the present study in Section 5.

2. The model

The half-doped manganite LCMO can be described as[8]

$$H = H_1 + H_2 + H_3 + H_4, \tag{1}$$

where H_1 describes the system with Jahn–Teller (JT) ions having an inter-play between electrons localized due to lattice distortions and those in the band states. This case is typical for manganites and can be described in terms of the Kondo-lattice model in the double exchange (DE) limit, taking into account the Jahn–Teller (JT) distortions and the super-exchange interaction between the localized electrons.[9] Then, following Ref. [10], we can divide e_g electrons into two groups: 'localized' electrons (l, $t^{(l)} \to 0$), which produce the maximal splitting of the e_g level, and itinerant 'band' electrons (c) with non-zero hopping integral t, leading to a smaller distortion of the MnO_6 octahedron. For simplicity of calculation, we assume that t does not change with θ_{ij} (the angle between local spins S_i and S_j), and then the Hamiltonian H_1 can be written as[9]

$$\begin{aligned} H_1 = & -t\sum_{\langle ij\rangle}\left(c_i^{\dagger}c_j + \text{h.c.}\right) - \varepsilon_{\rm JT}\sum_i n_{li} \\ & + J\sum_{\langle ij\rangle}\cos\theta_{ij} + U\sum_i n_{li}n_{ci}, \end{aligned} \tag{2}$$

*Project supported by the Priming Scientific Research Foundation of Changzhou University, China (Grant Nos. ZMF1002133 and ZMF09020023) and the National Natural Science Foundation of China (Grant No. 51202195).

†Corresponding author. E-mail: caoxs@nwpu.edu.cn

© 2013 Chinese Physical Society and IOP Publishing Ltd

where $\varepsilon_{\rm JT}$ is the JT energy gain for l electrons counting from the center of the c-electron band, J the exchange interaction energy, and U the Coulomb repulsion energy. Equation (2) describes the intra-atomic Hubbard interaction between the l electrons and l-c electrons, where $n_{li} = l_i^{\dagger} l_i$ and $n_{ci} = c_i^{\dagger} c_i$.

H_2 represents the lower e_g orbital (i.e., the one described by the operators c_k) and hybridizes with the localized t_{2g} orbitals (i.e., the operator l_k), which will modify the magnetic ordering of the t_{2g} electron. Thus the hybridization of the 'localized' electrons with conduction electrons is expressed as

$$H_2 = V \sum_k \left(c_k^{\dagger} l_k + l_k^{\dagger} c_k \right). \tag{3}$$

H_3 describes the electron–phonon interaction, and is written as

$$H_3 = \sum_i f(q) \left[c_{k+q}^{\dagger} l_k + l_{k+q}^{\dagger} c_k \right] \left(b_{-q}^{\dagger} + b_q \right), \tag{4}$$

where b_q ($b_q^{\dagger}$) is the annihilation (creation) operator for the phonon with wave vector q, and $f(q)$ is the electron–phonon coupling constant.

The free phonon Hamiltonian with phonon energy ω_q is written as

$$H_4 = \sum_q \omega_q b_q^{\dagger} b_q. \tag{5}$$

3. The phonon Green function and dielectric loss

The retarded phonon Green function is:

$$\begin{aligned} G^{\rm r}(t-t') &= \langle\langle A_q(t); A_{q'}(t') \rangle\rangle \\ &= -{\rm i}\Theta(t-t') \langle [A_q(t), A_{q'}(t')] \rangle, \end{aligned} \tag{6}$$

where

$$A_q = b_q + b_{-q}^{\dagger} \tag{7}$$

is the q-th Fourier component of the displacement. To derive the retarded phonon Green function $G^{\rm r}(t-t')$, we use the equation of motions for phonon operators

$${\rm i}\frac{{\rm d}A_q(t)}{{\rm d}t} = [A_q(t), H] = A_q(t) H - H A_q(t). \tag{8}$$

To Fourier transform the equation of motion, the retarded phonon Green function $G(\omega)$ is evaluated for the system using the total Hamiltonian H as given in Eq. (1). The retarded Green function is expressed as[11]

$$\begin{aligned} G^{\rm r}(\omega) &= \delta_{q,q'} D_q^0(\omega) + 4 f^2(-q) D_q^0(\omega) \\ &\quad \times \chi_{q,q'}(\omega) D_q^0(\omega), \end{aligned} \tag{9}$$

where

$$D_q^0(\omega) = 2\omega_q \left[\omega^2 - \omega_q^2 \right]^{-1} \tag{10}$$

is the free phonon propagator, and $\chi_{q,q'}(\omega)$ is the electron response function. Applying the Dyson approximation to Eq. (9), the retarded phonon Green function can be written as

$$G^{\rm r}(\omega) = 2\omega_q \left[\omega^2 - \omega_q^2 - \Sigma_q(\omega) \right]^{-1}. \tag{11}$$

In the cases of long wavelength and finite temperature, the retarded phonon Green function is written as

$$G^{\rm r}(\omega, q=0) = \frac{\omega_0}{\omega^2 - \omega_0^2 - \Sigma(\omega, q=0)}. \tag{12}$$

The phonon self-energy is

$$\Sigma(\omega, q=0) = -8 g \omega_0^2 I, \tag{13}$$

where

$$\begin{aligned} I &= \int_{-W/2}^{W/2} \frac{{\rm d}\varepsilon_k}{|D|} I_1, \\ I_1 &= 2\frac{(E_k - E_0)}{\omega_1 - \omega_2} \left[f(\omega_1) - f(\omega_2) \right], \\ |D| &= \left[\omega^2 - (E_k - E_0)^2 - 4V^2 \right], \\ \omega_{1,2} &= \Big(\varepsilon_k + \varepsilon_{\rm JT} + 0.5U \\ &\quad \pm \sqrt{[\varepsilon_k - \varepsilon_{\rm JT} + U(2n_l - 0.5)]^2 + 4V^2} \Big) \Big/ 2, \\ n_l &= \frac{1}{\omega_1 - \omega_2} [(\omega_1 - \varepsilon_k - U n_l) f(\omega_1) \\ &\quad - (\omega_2 - \varepsilon_k - U n_l) f(\omega_2)]. \end{aligned} \tag{14}$$

The dielectric loss ($\tan\delta$) is defined as the ratio between imaginary $G^{\rm r}_{\rm imaginary}(\omega)$ part and real $G^{\rm r}_{\rm real}(\omega)$ part of dielectric constant and can be written as[12,13]

$$\tan\delta = G^{\rm r}_{\rm imaginary}(\omega) / G^{\rm r}_{\rm real}(\omega). \tag{15}$$

4. Results and discussion

The parameter $g = N(0) f^2(0)/\omega_0$ is the phonon coupling to the hybridization between the l electrons and the conduction electrons, where $N(0)$ is the density of states of the conduction electrons at the Fermi level ($\varepsilon_{\rm F}$), parameter ω_0 is the soft-mode frequency of the pure harmonic, and ω is the microwave frequency.

Figures 1–3 show the variations in the dielectric loss $\tan\delta$ with temperature T for different values of $\varepsilon_{\rm JT}$, U, and g at the fixed values of frequency $\omega_0 = 5.0$ and $\omega = 8.0$. The first important feature of these curves is that there is a peak in the $\tan\delta$ at $T_{\rm CO}$. The second is the absence of any large anomaly in $\tan\delta$ at the magnetic transitions. Similar results have also been reported in experiments with other perovskite-type ferroelectric oxide materials.[14–18]

The CO transition in the LCMO is found to be accompanied by a structural transition from an orthorhombic phase with a space group *Pnma* to a lower symmetry monoclinic phase with $P2_1/m$ space group.[19] The space group accounts for the two inequivalent sites for the Mn^{3+} and Mn^{4+} ions,

which are created as a result of charge ordering, leading to a highly distorted octahedron. In this model, the Mn oxidation state is constant (+3.5) and the supernumerary electron relates to the DE Zener mechanism and ferromagnetically couples the Mn ions in pairs, resulting in the Zener polaron.[19] While Komskii *et al.*[20] argued that the Zener polaron state may be favored in a certain part of the phase diagram in these compound systems. In this case, a net polarization appears due to the favoring of a ferroelectric state. In such a scenario, an anomaly on the dielectric loss at the charge ordering temperature is expected.

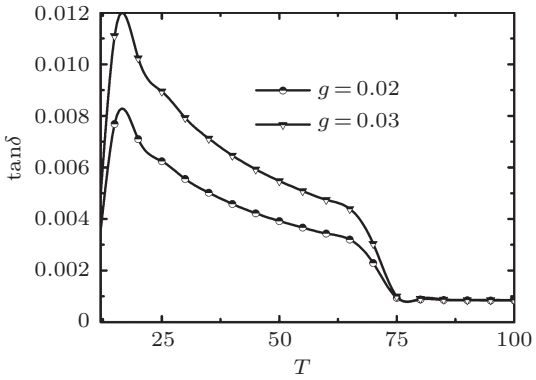


Fig. 1. The temperature-dependence of the dielectric loss at two different values of electron–phonon coupling parameter g.

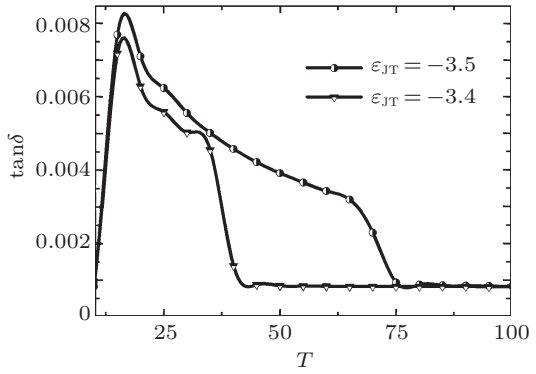


Fig. 2. The temperature-dependence of the dielectric loss at two different positions of the bare l-level $\varepsilon_{\rm JT}$.

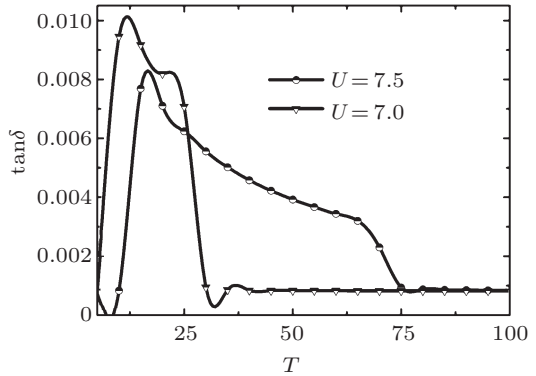


Fig. 3. The temperature-dependence of the dielectric loss at two different values of Coulomb interaction U.

Figure 1 describes the temperature-dependence of the dielectric loss at the different strengths of phonon coupling to the hybridization between the l electrons and conduction electrons (g). Since the phonon is coupled to the weak hybridization between the conduction electrons and l electrons, the electron–phonon coupling parameter g is small in magnitude.

It is observed that the peak intensity increases with increasing g. The increase in g means that the electron–phonon coupling increases, which causes the distortion of the lattice to increase, and the dielectric loss shows enhanced intensity. As is well known, the longitudinal phonon is always accompanied by the change in crystal volume and local lattice constant. (The electron–phonon coupling deformation potential is $\delta\varepsilon_c = c_1\Delta(r)$, where $\delta\varepsilon_c$ is the deformation potential, c_1 a constant, and $\Delta(r)$ the volume change[21]). These can also be found in Ref. [5].

It can be observed from Fig. 2 that the peak intensity increases with increasing $|\varepsilon_{\rm JT}|$. In addition to strong electron phonon interactions, the JT lattice distortions lead to a canting instability of the antiferromagnetic (AFM) state. This behavior favors the formation of spin dimers that drive charge ordering from site-centered to bond-centered, leading to the appearance of ferroelectric properties in the charge ordered manganites.[6]

Figure 3 shows the plots of tanδ versus T for two different values of the Coulomb interaction, i.e., $U = 7.5$ and 7.0 with fixed values of $\varepsilon_{\rm JT} = -3.5$, $V = 0.5$, and $g = 0.02$. It is found that the peak intensity decreases with increasing U. From the above discussion, it is found that the Coulomb interaction has an influence on the peak position of the dielectric loss and the peak intensity. As U increases, the DE ferromagnetic (FM) interaction increases, while the AFM and electron–phonon interaction decreases. The increase in W (electron e_g band width) favors electron transfer and hence the FM interaction.[22] This is the reason for the peak positions of the dielectric loss shifting toward high temperature, while the peak intensity decreases as U increases.

5. Conclusions

In this paper, the dielectric loss tanδ of the LCMO is studied using the quantum microscopic model. It is found that at the AFM–CO transition temperature, the dielectric loss presents a sharp peak, and it is observed that the transition temperature $T_{\rm P}$ rises as $|\varepsilon_{\rm JT}|$ and U increase. It is also found that the peak intensity of tanδ decreases with increasing U. It is worth noting that $T_{\rm P}$ remains unchanged and the strength of tanδ is augmented with increasing g. These results are consistent with the experimental results.[4] Electronic phase separation is invoked as one possibility to explain the observed dielectric behavior of these manganites. The coexistence of FM (metallic) and CO AFM (insulating) regions in the solid could

increase the capacitive response of the system, as reported in several studies dealing with metallic particles embedded in insulating matrices.[23] This behavior is controlled by the volume fraction of the metal in the composite. For LCMO, the fraction of the FM region strongly depends on temperature, as reported experimentally in Ref. [24].

References

[1] Claude Ederer and Nicola A Spaldin 2004 *Nat. Mater.* **3** 849
[2] Rivas J, Rivas-Murias B, Fondado A, Mira J and Señarís-Rodríguez M A 2004 *Appl. Phys. Lett.* **85** 6224
[3] Paolo Barone, Silvia Picozzi and Jeroen van den Brink 2011 *Phys. Rev. B* **83** 233103
[4] Zou T, Wang F, Liu Y, Yan L Q and Sun Y 2010 *Appl. Phys. Lett.* **97** 092501
[5] Indu Dhiman, Deshpande S K and Das A 2010 *J. Appl. Phys.* **108** 083915
[6] Giovannetti G, Kumar S, Brink J and Picozzi S 2009 *Phys. Rev. Lett.* **103** 037601
[7] Silvia Picozzi1, Kunihiko Yamauchi1, Ivan A Sergienko, Cengiz Sen, Biplab Sanyal and Elbio Dagotto 2008 *J. Phys.: Condens. Matter* **20** 434208
[8] Cao X S and Chen C L 2008 *Phys. Lett. A* **372** 5356
[9] Kugel K I, Rakhmanov A L and Sboychakov A O 2005 *Phys. Rev. Lett.* **95** 267210
[10] Ramakrishnan T V, Krishnamurthy H R, Hassan S R and Pai G V 2004 *Phys. Rev. Lett.* **92** 157203
[11] Elk K 1974 *Phys. Stat. Sol. (b)* **64** 489
[12] Kubo R 1957 *J. Phys. Soc. Jpn.* **12** 570
[13] Zubarev D N 1960 *Phys. Usp.* **3** 320
[14] Chang F G, Song G L, Fang K and Wang Z K 2007 *Acta Phys. Sin.* **56** 6068 (in Chinese)
[15] Zhang C H, Xu Z, Gao J J and Wang B K 2009 *Acta Phys. Sin.* **58** 6500 (in Chinese)
[16] Guo X,Wang X, Zheng W and Tang W H 2010 *Acta Phys. Sin.* **59** 2815 (in Chinese)
[17] Wang W, Wang X J, Zhu J, Mao X Y and Chen X B 2009 *Chin. Phys. Lett.* **26** 047701
[18] Shah M R and Akther Hossain A K M 2012 *Chin. Phys. Lett.* **29** 047803
[19] Mercone S, Wahl A, Pautrat A, Pollet M and Simon C 2004 *Phys. Rev. B* **69** 174433
[20] Khomskii D, Dmitry V Efremov, Jeroen van den Brink and Daniel I Khomskii 2003 arXiv: 0306651v1 [cond-mat. str-el]
[21] Bardeen J and Shockley W 1950 *Phys. Rev.* **80** 72
[22] Sundaresan A, Paulose P L, Mallik R and Sampathkumaran E V 1998 *Phys. Rev. B* **57** 2690
[23] Pecharromán C and Moya J S 2000 *Adv. Mater.* **12** 294
[24] Rivadulla F, Freita-Alvite M, López-Quintela A, Hueso L E, Miguéns D R, Sande P and Rivas J 2002 *J. Appl. Phys.* **91** 785